A&A manuscript no.
(will be inserted by hand later)

Your thesaurus codes are:
03 08.16.6; 08.14.1; 08.02.3;

ASTRONOMY AND ASTROPHYSICS

February 1, 2008

The X-ray emission properties of millisecond pulsars

W. Becker and J. Trümper

Max-Planck-Institut für extraterrestrische Physik, D-85740 Garching bei München, Germany

Received: March 6. 1998 / Accepted May 15. 1998

Abstract. Until now X-radiation from nine millisecond pulsars has been detected. In the present paper we summarize the observations and show the results of a reanalysis of archival ROSAT data. In addition we present the results of recent observations of PSR J0437−4715 with the ROSAT PSPC and HRI detectors. We show that the pulsed fraction is independent of energy in the range 0.1−2.4 keV. The pulse width as measured at X-ray energies is comparable with that observed in the radio domain. An upper limit for the X-ray luminosity of the pulsar's bow-shock visible in H_α is found to be $L_x < 2 \times 10^{29}\,\mathrm{erg\ s^{-1}} (d/180\mathrm{pc})^2$. We further report on the discoveries of PSR J1024−0719, J1744−1134 and J2124−3358 with the ROSAT-HRI, making them the first solitary galactic millisecond pulsars detected at X-ray energies. The pulse profile of PSR J2124−3358 shows marginal evidence for a double peak structure. We finally discuss the observed emission properties of the detected millisecond pulsars and conclude that the measured power-law spectra and pulse profiles together with the close correlation between the pulsar's spin-down energy $\dot{E}$ and the observed X-ray luminosity suggests a non-thermal origin for the bulk of the observed X-rays.

Key words: Pulsars: individual (PSR B1821-24, J0218+4232, B1957+20, J0437-4715, J1012+5307, J1024-0719, J1744-1134, J2124-3358, J0751+1807) – X-rays: general – Stars: neutron – Stars: binaries: general – Clusters: globular

1. Introduction

The satellite observatories ROSAT, ASCA and EUVE have brought important progress in neutron star and pulsar astronomy. With significantly higher sensitivities compared with previous X-ray satellites they allowed for the first time the detection of X-ray emission from objects as faint as millisecond pulsars.

Send offprint requests to: W. Becker
Correspondence to: web@mpe.mpg.de

Millisecond pulsars form a separate group among the rotation-powered pulsars.They are distinguished by their small spin periods ($P \leq 20$ ms) and high spin stability ($dP/dt \approx 10^{-18} - 10^{-21}$ s/s). Consequently, they are very old objects with spin-down ages $P/2\dot{P}$ of typically $10^9 - 10^{10}$ years and magnetic dipol components $B_\perp \propto \sqrt{P\,\dot{P}}$ of the order of $10^8 - 10^{10}$ G (see Taylor et al. 1995). More than $\sim 75\%$ of the known disk millisecond pulsars are in binaries with a compact companion star, compared with the $\cong 1\%$ of binary pulsars found in the general population. This gives support to the idea that their fast rotation has been acquired by angular momentum transfer during a past mass accretion phase (Bisnovatyi-Kogan & Komberg 1974; Alpar et al. 1982; Bhattacharya & Van den Heuvel 1991; Urpin et al. 1998; see also the recent results by Wijnands & Van der Klis (1998) on SAX 1808.4-3658).

Before the launch of ROSAT, nothing was known on the X-ray emission properties of millisecond pulsars. According to the standard models of cooling neutron stars, millisecond pulsars are too old to expect detectable thermal emission (see Tsuruta 1998 and references therein). Thermal X-ray emission, however, may be emitted from polar caps heated up to temperatures of few million degrees by high energy secondary $e^\pm$ streaming back to the neutron star's polar cap regions (Arons 1981; Kundt & Schaaf 1993; Gil & Krawczyk 1996). Non-thermal processes, which may account for the X-ray emission from millisecond pulsars, are: magnetospheric emission from relativistic particles, characterized by a power-law spectrum; X-rays from a relativistic pulsar wind or from an interaction of that wind with the interstellar medium or a close companion star (Arons & Tavani 1993).

At present, there are 33 rotation-powered pulsars detected in the soft X-ray domain (see Becker & Trümper 1997 and references therein)[1]. Nine of them belong to the group of millisecond pulsars. In this paper we review the recent millisecond pulsar observations at X-ray energies and report on results obtained with the ROSAT, EUVE,

[1] Updated versions of the Tables 1 and 3 from Becker & Trümper (1997) are available online from the URL http://www.xray.mpe.mpg.de/∼web/bt97_update.html.

ASCA and RXTE satellites. The structure of the paper is as follows: After a brief description of the analysis techniques in Sect. 2 we summarize the X-ray emission properties of the faint detections (PSR 1957+20, J0751+1807, J1012+5307, J1024−0719 and J1744−1134) in Sect. 3. Results from the nearby and bright pulsar PSR J0437−4715 are presented in Sect. 4. In chapter 5 and 6 we summarize recent results obtained from the globular cluster pulsar PSR 1821−24 and from PSR J0218+4232. The discovery of pulsed X-ray emission from the solitary galactic millisecond pulsar PSR J2124−3358 and the conclusions are presented in Sect. 7 and Sect. 8.

2. Data analysis

The ROSAT data presented in this paper were analyzed using the extended scientific analysis software EXSAS (Zimmermann et al. 1994). Source positions and count rates were obtained from a maximum likelihood analysis of the source photons in combination with a spline fit to the background after removing solar-scattered X-rays and the particle background. Count rates were dead-time and vignetting corrected.

Five of the nine millisecond pulsars detected by ROSAT are identified only by positional coincidence with the pulsar's radio position (see Sect. 3). With about $10 - 80$ source counts the data of these pulsars do not allow a spectral analysis. Two other millisecond pulsars (PSR J0218+4232 and J2124-3358) are detected by the ROSAT HRI only, which does not provide spectral information. Nevertheless, an estimate for the pulsar's energy flux and luminosity within 0.1−2.4 keV can be obtained from the observed count rate with only few additional assumptions: the pulsar's X-ray spectrum, its distance and the absorption column N_H. Detailed information on the X-ray spectrum is only available for two (PSR J0437−4715, PSR 1821−24) of the nine detected millisecond pulsars. In both cases the best fitting spectral model implies a power-law nature for the emitted X-radiation. Becker & Trümper (1997) have shown recently that with the exception of the younger pulsars Crab, B1509−58 and the Vela pulsar all pulse-phase averaged photon indices measured for rotation-powered pulsars in the soft X-ray domain are consistent with a photon-index $\alpha \approx -2$. Calculating luminosities we therefore use the individual photon indices resulting from spectral fits and a *canonical* value of $\alpha = -2$ where no spectral information is available. The proper motion corrected period derivatives were used to compute $\dot{E}$, $B_\perp$ and the spin-down age τ for PSR 1957+20 (Camilo et al. 1994), PSR J0437−4715 (Bell et al. 1995; Sandhu et al. 1997) and PSR J2124−3358 (Bailes et al. 1997).

The ROSAT PSPC and HRI temporal resolution of 130 μs and 64 μs, respectively, is sufficient to resolve X-ray pulses from millisecond pulsars. A low number of detected source photons does not necessarily preclude a search for pulsation. For instance, *evidence* for pulsed X-ray emission was found in the ROSAT all-sky survey data of PSR J0437−4715 already with a number of ~ 50 source counts (Becker et al. 1993a). For the reduction of the photon arrival times from the spacecraft coordinates and recorded times to the solar system barycenter and the barycentric dynamical time-scale (TDB), we performed the standard procedures for ROSAT data (see Becker et al. 1993b) using the JPL DE200 Earth ephemeris and the pulsar ephemeris valid for the observational epoch. Correction of the photon arrival times for a pulsar's binary motion was performed using the method of Blandford & Teukolsky (1976).

Millisecond pulsars are stable clocks. Given the high precision of the pulsar's radio ephemeris, each X-ray photon arrival time can be directly related to the pulsar's rotation phase ϕ using the relation ϕ_i = fractional part of $(f\Delta t_i + \frac{1}{2}\dot{f}\Delta t_i^2)$ with $i = 1$ to N, where N is the number of photons, f and $\dot{f}$ the pulsar frequency and its first time derivative at the reference epoch t_{ref} and $\Delta t = t_i - t_{ref}$. The statistical significance for pulsations was computed using the Z_n^2-test with $n = 1$ to 10 harmonics in combination with the H-Test to determine the optimal number of harmonics in the periodic signal (De Jager 1987; Buccheri & De Jager 1989).

Various methods have been employed to measure the fraction of pulsed photons: approaches like fitting sinusoids to the phase histogram using the Rayleigh-Power or estimating the minimum in a light curve to find the DC-level are often valid only for specific pulse shapes (e.g. real sinusoids) or completely neglect random fluctuations around the lowest level. An additional dependence on the number of bins used for the pulse phase histogram, makes the pulsed fraction often a rather method dependent estimate. To avoid these problems we have computed the pulsed fractions by using a bootstrap method. This approach has been recently used by Swanepoel et al. (1996) in the analysis of gamma-ray pulsars. The advantage of this method is that the fraction of pulsed photons is calculated from the data without having to construct a histogram or any other estimate of the light curve.

Another concern is the number of phase bins used to construct pulse profile histograms for presentation purposes or for comparison with model light curves. Here, the bin width is limited on one side by the instruments temporal resolution but on the other side also by the statistical significance of the signal. The latter is often not taken into account. In this work we have chosen the number of phase bins to construct a pulse profile histogram by using the following approach: denoting the Fourier-power of the i-th harmonic by R_i and taking m as the optimal number of harmonics as deduced from the H-test, an exact

expression for the optimal number of phase bins is given by (De Jager 1998, in prep.)

$$M = 2.36 \left(\sum_{i=1}^{m} i^2 R_i^2 \right)^{1/3} \quad (1)$$

This expression compromises between information lost due to binning (i.e. zero bin width to get all information), and the effect of fluctuations due to finite statistics per bin (i.e. bin width as large as possible to reduce the statistical error per bin). The total error (bias plus variance) is minimized at a bin width of $1/M$.

3. The faint detections

3.1. The black-widow pulsar: PSR B1957+20

The first millisecond pulsar reported in X-rays was the so called black-widow pulsar, a 1.6 ms pulsar at a distance of 1.53 kpc, which is in a close, approximately 9.16h orbit with a low-mass white dwarf companion of ~ 0.025 $M_\odot$ (Fruchter et al. 1988). The source was observed in October 1991 with both the PSPC and the HRI detector. We have reanalyzed the archival ROSAT data (Rev 2) and found the source detected in the PSPC observation with a total of 82 counts of which $\approx$ 18 counts belong to the background. With an exposure time of 15 511s we deduce a PSPC count rate of $(4.2 \pm 0.6) \times 10^{-3}$ cts/s in 0.1−2.4 keV, approximately twice the number given by Kulkarni et al. (1992) for the range 0.5-2.0 keV. The pulsar is marginally detected in the HRI data, in agreement with the results presented by Fruchter et al. (1992). An estimate of the pulsar's X-ray flux from the count rate results in $f_x = 3 \times 10^{-13}$ erg s^{-1}cm^{-2}, implying a luminosity of $L_x = 8.5 \times 10^{31} (d/1.53 \text{ kpc})^2$ erg s^{-1} and an X-ray efficiency of $L_x/\dot{E} \approx 0.8 \times 10^{-3}$. For the interstellar absorption we have adopted $N_H \approx 4.5 \times 10^{21}$ cm^{-2} as estimated by Kulkarni et al. (1992) from the visual extinction ($A_v \approx 1-2$) of a star close to the pulsar position (see Djorgovski & Evans 1988).

To search for a modulation of the detected X-rays at the pulsar's rotation period, a photon arrival time analysis was applied to all photons selected from a 35 arcsec aperture centered on the pulsar's X-ray position. The selected counts represent more than 99.9% of the PSPC source photons with a background contribution of about 15%. Folding the corrected arrival times according to the pulsar ephemeris valid for the ROSAT observational epoch did not reveal significant X-ray pulses. A not very restrictive 1σ upper limit of 60% has been deduced for the X-ray pulsed fraction.

Arons & Tavani93 (1993) have proposed that X-ray emission from PSR 1957+20 could arise from the pulsar itself or from the pulsar wind which is evaporating the companion star. The low number of counts recorded from this pulsar does not allow us to distinguish between the two mechanisms.

3.2. PSR J0751+1807

This binary pulsar has been recently discovered by Lundgren et al. (1995) in the error box of the unidentified EGRET source CGRO J0749+1807 (Hartman et al. 1992; Fichtel et al. 1993) but the association between the pulsar and the putative gamma-ray source could not be established (CGRO J0749+1807 is of marginal significance only and was finally removed from the 2EG and 3EG catalog of gamma-ray sources (Thompson et al. 1995; Hartman et al. 1998)). The 3.48 ms pulsar and its low-mass white dwarf companion are in a circular 6.3h orbit. The dispersion measure based pulsar distance is 2 kpc.

ROSAT observed the pulsar in November 1993 (13 992s, on-axis) and April 1994 (7008s, 37 arcmin off-axis) with the PSPC (Becker et al. 1996). Approximately 50 source counts were recorded in the November 93 observation leading to a PSPC count rate of $(3.6 \pm 0.6) \times 10^{-3}$ cts/s. The degradation of the PSPC's point source sensitivity at 37 arcmin off-axis in combination with a reduced exposure time prevented a detection of the pulsar in the April 94 data. Estimating the pulsar's X-ray flux and luminosity from the 1993 PSPC count rate yields $f_x = 8.3 \times 10^{-14}$ erg s^{-1}cm^{-2} and $L_x = 4 \times 10^{31} (d/2 \text{ kpc})^2$ erg s^{-1}, implying an X-ray efficiency of $L_x/\dot{E} \approx 5.3 \times 10^{-3}$. Converting the count rate to an energy flux is very sensitive to the assumed interstellar absorption. The pulsar's dispersion measure implies a value of 9×10^{20} cm^{-2}, making the usual but uncertain assumption that there are 10 hydrogen atoms for each free electron along the line of sight. The model of Dickey & Lockman (1990) implies $N_H \sim 5 \times 10^{20}$ cm^{-2} for the total hydrogen column through the Galaxy whereas from the HI survey of Stark et al. (1992) we deduce $N_H \sim 4 \times 10^{20}$ cm^{-2}. The latter is adopted for the pulsar's absorption column.

A timing analysis did not reveal significant X-ray pulses at the expected radio period. A 1σ upper limit of 70% is deduced for the fraction of pulsed photons.

3.3. PSR J1012+5307

PSR J1012+5307 is a 5.26 ms pulsar which is in a 14.5h binary orbit with a low-mass white dwarf companion. The pulsar was discovered recently during a survey for short-period pulsars using the Lovell radio telescope at Jodrell Bank (Nicastro et al. 1995). A detection of the companion star at optical wave-length was reported from an inspection of the Palomar sky survey plates by the same authors. The distance of the pulsar as estimated from its dispersion measure is 0.52 kpc.

A marginal X-ray detection of PSR J1012+5307 was reported recently by Halpern (1996) who found the millisecond pulsar $\approx 30'$ off-axis in a serendipitous PSPC observations of approximately 14.5 ksec duration. An excess of $\approx 80 \pm 20$ counts above the background level within a circle of 2.5′ and within 1′ of the pulsar's radio posi-

tion has been interpreted as a possible detection of the pulsar (Halpern 1996). Converting the PSPC count rate to an energy flux we find $f_x = 4.9 \times 10^{-14}$ erg s^{-1}cm^{-2} and $L_x = 1.6 \times 10^{30} (d/0.52 \text{ kpc})^2$ erg s^{-1} for the X-ray luminosity within 0.1−2.4 keV. The latter implies an X-ray efficiency of $L_x/\dot{E} \approx 0.4 \times 10^{-3}$. For the interstellar absorption we used $N_H = 7 \times 10^{19}$ cm^{-2} as given by Snowden et al. (1994) for the HI hole in Ursa Major. No X-ray pulses have been detected from PSR J1012+5307. A 1σ pulsed fraction upper limit is 75%. A 100 ksec ROSAT HRI observation to confirm the pulsars X-ray detection is scheduled for the second half of 1998.

3.4. PSR J1024−0719 and J1744−1134

At present there are only nine galactic millisecond pulsars which are not in binary systems (Camilo 1996). PSR J1024−0719 and J1744−1134 are two of them. Both pulsars were discovered recently by Bailes et al. (1997) during the Parkes 436 MHz survey of the southern sky. PSR J1024−0719 has a rotation period of 5.16 ms and a period derivative of $\dot{P} = 1.84 \times 10^{-20}$ s s^{-1}, implying an upper limit to the pulsar age of $\geq 4.4 \times 10^9$ years and a rotational energy loss of $\geq 5.3 \times 10^{33}$ erg s^{-1}. The spin parameters of PSR J1744−1134 are similar to those of J1024−0719: with a period of 4.07 ms and a period derivative of 0.86×10^{-20} s s^{-1} the pulsars spin-down age is $\geq 7 \times 10^9$ years and the spin-down energy is $\geq 1.42 \times 10^{33}$ erg s^{-1}. We note that for both pulsars the Shklovskii contribution to $\dot{P}$ is not well constrained so far (see Bailes et al. 1997). The spin-down age and the rotational energy loss given above are preliminary for that reason.

Both millisecond pulsars are at a relative close distance to us. For PSR J1024−0719 the Taylor & Cordes model implies $d \sim 350$ pc based on the pulsar's dispersion measure (Bailes et al. 1997), whereas for PSR J1744−1134 the radio parallax has been measured recently and yielded a distance of about 260 ± 60 pc (Bailes 1997, priv. comm.).

ROSAT HRI observations of PSR J1024−0719 and J1744−1134 were performed in November/December and September 1997 for an effective exposure time of 80 635 sec and 61 238 sec, respectively. The X-ray sources RX J1024.6−0719 (RA=10:24:38.60, DEC=−07:19:21.5) and RX J1744.4−1134 (RA=17:44:29.35, DEC=−11:34:52.2) were detected with a significance of $\sim 4-5\sigma$, only 2−3 arcsec distant from the pulsars' positions (Becker & Trümper 1998; Becker et al. 1998, see Fig.1). The positional offset between RX J1024.6−0719, RX J1744.4−1134 and the pulsars' radio position is well within the uncertainty of the satellite pointing accuracy. The probability that RX J1024.6−0719 and RX J1744.4−1134 are chance superpositions of unrelated background object is $\sim 10^{-4}$ and $\sim 3 \times 10^{-5}$, respectively, estimated from the density of X-ray sources in the HRI field of view. We therefore accept RX J1024.6−0719 and RX J1744.4−1134 as the likely X-ray counterparts of the millisecond pulsars PSR J1024−0719 and J1744−1134.

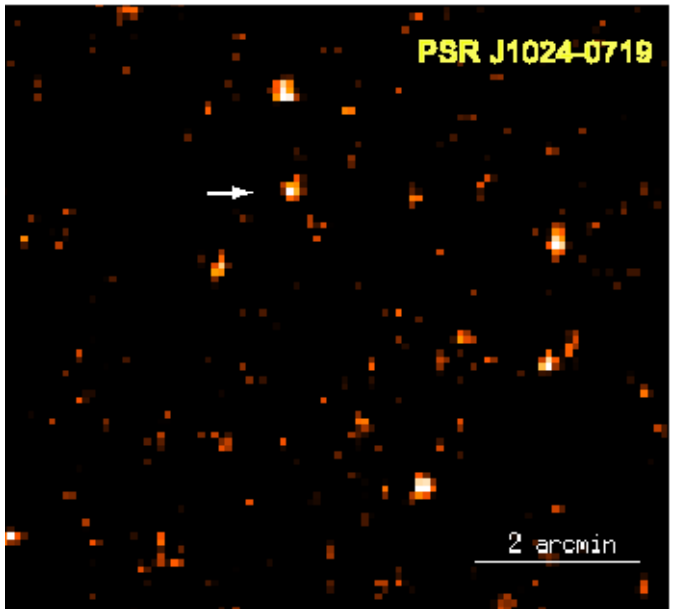

Fig. 1. Sub-image of the PSR J1024−0719 field as observed with the ROSAT HRI in November/December 1997. The image has a spatial binning of 5 arcsec. The pulsar's X-ray counterpart RX J1024.6−0719 is indicated by an arrow. Several unidentified X-ray sources are detected in the pulsar's neighborhood, only few arcmin distant from the pulsar

Converting the HRI source count rate of $(3.3 \pm 0.9) \times 10^{-4}$ and $(2.9 \pm 0.9) \times 10^{-4}$, as deduced for J1024−0719 and J1744−1134, to an energy flux we find $f_x \sim 2 \times 10^{-14}$ erg s^{-1}cm^{-2} within 0.1−2.4 keV for both sources. The latter implies an X-ray luminosity of $L_x = 3 \times 10^{29} (d/0.35 \text{ kpc})^2$ erg s^{-1} and $L_x = 2 \times 10^{29} (d/0.26 \text{ kpc})^2$ erg s^{-1} for J1024−0719 and J1744−1134. For the interstellar absorption we used $N_H = 2 \times 10^{20}$ cm^{-2} and 10^{20} cm^{-2} respectively, as deduced from the pulsars' dispersion measure. The number of recorded counts was not sufficient to perform a search for pulsations.

4. The nearby and bright pulsar PSR J0437-4715

The first millisecond pulsar for which a more detailed knowledge of its X-ray emission properties has become available is the 5.75 ms pulsar PSR J0437−4715. The source, which was discovered in the Parkes southern sky survey by Johnston et al. (1993) and which is in a close 5.74-day circular orbit around a ≈ 0.25 M$_\odot$ white-dwarf companion (Johnston et al. 1993; Becker et al. 1993a; Bailyn 1993; Danziger et al. 1993) is the nearest and brightest millisecond pulsar known. Recent measurements of the annual parallax have adjusted the pulsar's distance to be 178 ± 26 pc

(Sandhu et al. 1997), placing it somewhat further away than originally indicated by the dispersion measure and the electron density model of Taylor & Cordes (1993). The parallax distance further constrains the pulsar's proper motion and revises its intrinsic period derivative down to $\dot{P}_{int} = (0.8 \pm 0.7) \times 10^{-20}$, approximately a factor of 7 smaller than the observed one $\dot{P}_{obs} = 5.73 \times 10^{-20}$ (Bell et al. 1997). Based on $\dot{P}_{int}$ the pulsar's spin-down energy and polar magnetic field is found to be $\log \dot{E} = 33.22^{+0.3}_{-0.9}$ erg/s and $\log B_{\perp} = 8.34^{+0.13}_{-0.44}$ G, respectively. The pulsar's characteristic age is $P/2\dot{P}_{int} \lesssim 6 \times 10^9$ yr.

X-ray emission from the pulsar was first detected in the ROSAT all-sky survey by Becker et al. (1993a). Based on a serendipitous ≈ 6 ksec pointed observation with the ROSAT PSPC Becker & Trümper (1993) found that the X-ray emission is pulsed and the pulsar's soft X-ray spectrum is best described by a single power-law. An energy dependent pulsed fraction showing a peak at ~ 0.9 keV was found by fitting a sine wave to the X-ray pulse profiles obtained for different energy ranges. Because it appeared difficult to explain this apparent energy dependence in terms of single-component emission Becker & Trümper (1993) proposed that the radiation from PSR 0437−4715 is a mixture of spin-modulated thermal emission from heated polar caps combined with unpulsed emission from a pulsar wind or plerion. A reanalysis of the serendipitous ROSAT data together with data taken with the EUVE satellite at 65 − 120 Å (Halpern et al. 1996) confirmed the results of Becker & Trümper (1993) but has weakened the case of an energy dependence of the pulsed fraction by using improved pulsar ephemeris and a different method to estimate the fraction of pulsed photons.

In the following we present the results from a reanalysis of the archival ROSAT data of PSR 0437−4715 including unpublished data from subsequent observations with both the ROSAT PSPC and HRI detectors.

4.1. Observations

Since its discovery in 1993, PSR J0437−4715 has been the target of several pointings with both the PSPC and the HRI. A total of ~ 20 ksec PSPC observations and ~ 60 ksec HRI observations have been performed with different sensitivities. The coverage of the pulsar's binary orbit by ROSAT observations is illustrated in Fig. 2.

Pointed observations with the ROSAT PSPC were performed on 1992, September 20−21 for an effective exposure time of 5846 s and on 1994 July 2−4 for 9885 s and 4459 s, respectively. The latter observation was done with the boron filter. As a consequence, the pulsar's PSPC count rate is reduced to 0.042 ± 0.003 cts/s, compared with a count rate of 0.204 ± 0.005 cts/s for the filter-off observation. In addition, ROSAT observations with the HRI were performed between 1994 July 18th and August 24th and on 1997 September 22−26 for an effective exposure time of 35 209 and 22 928 seconds, respectively. In the later observation the satellite wobble-mode was disabled. The pulsar's HRI source count rate is 0.042 ± 0.002 cts/s.

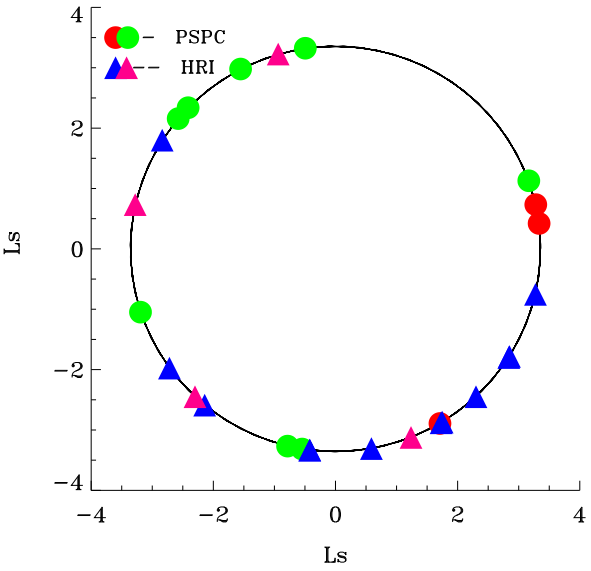

Fig. 2. Coverage of the pulsar's binary orbit by X-ray observations using ROSAT. Circles indicate observations with the PSPC in the focus of the telescope whereas triangles represent HRI observations.

4.2. Spatial emission properties of PSR J0437−4715

PSR J0437−4715 is one of few millisecond pulsars for which an H_α bow-shock nebula has been detected (Bell et al. 1993; 1995). Others are the black-widow pulsar PSR 1957+20 (Kulkarni & Hester 1989) and PSR J2225+6535 which is surrounded by the so called Guitar Nebula (Cordes et al. 1993; Romani et al. 1997). It is generally believed that the pulsar wind, a mixture of charged particles and electromagnetic radiation, shocks the interstellar medium (see Arons & Tavani 1993) giving rise to a bow-shock. Such a shock region can produce both thermal emission and synchrotron radiation. Only the local conditions, such as the magnetic field and particle density, determines if X-rays are produced and which emission process dominates.

The optical bow-shock nebula of PSR J0437-4715 has a standoff distance from the pulsar position of about 12 arcsec (see Fig.3). Diffuse optical emission of the nebula is visible up to about 1 arcmin from the pulsar position along the side wings of the bow-shock hyperboloid. The pulsar's proper motion direction is $122° \pm 2°$ (Bell et al. 1995), measured anticlockwise from north.

With a spatial resolution of ~ 25 arcsec (FWHM) PSR J0437−4715 appears to be point like in the available PSPC data. A source extension at energies below ~ 0.2 keV is found to be caused by the well known ghost imaging effect,

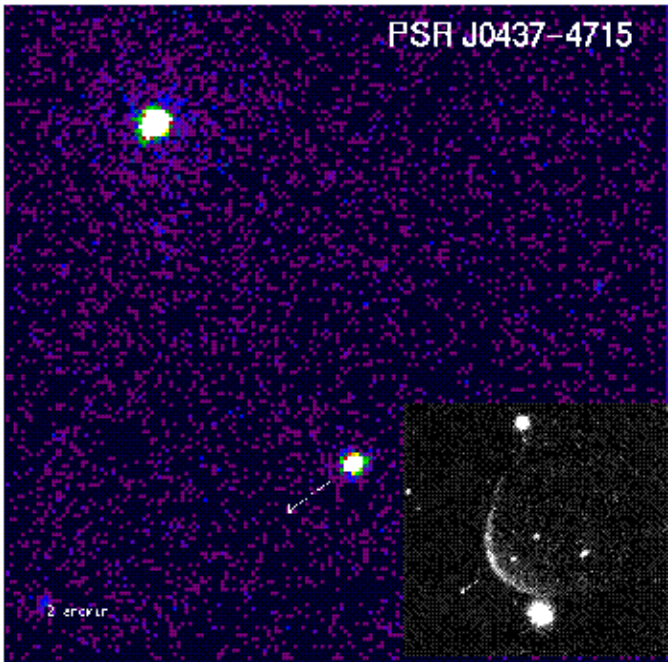

Fig. 3. Sub-image of the pulsar field as observed with the ROSAT HRI in September 1997 (satellite wobble disabled). The image has a spatial binning of 2.5 arcsec. The 4.3 arcmin neighboring source RX J0438.1-4710, identified to be a Seyfert 1 Galaxy at $z = 0.051$ (Grupe 1996) is visible to the upper left. The inset in the lower right corner shows the pulsar's optical bow-shock nebula as observed by A. Fruchter in H_α. The arrow indicates the pulsars proper motion direction, which has an orientation of $\sim 122°$ measured anticlockwise from north.

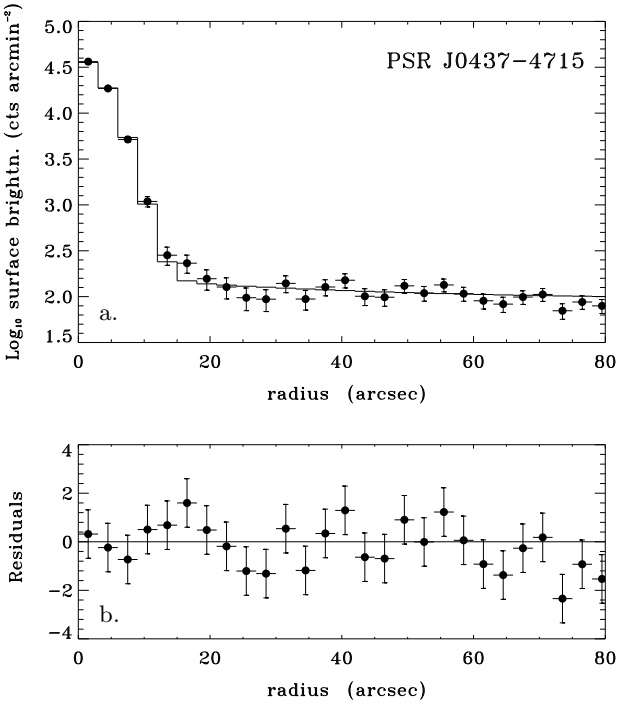

Fig. 4. a. The radial surface brightness distribution within an 80 arcsec circle centered on the pulsar PSR J0437−4715 and based on the 1997 HRI data. The histogram incorporates a point source and an additional broadening of the PSF to account for an uncorrected 2.6 arcsec attitude error, smearing out the model point spread function. **b.** Residuals of the PSF fit in units of σ. The fit has a reduced χ^2 of 0.87.

an instrumental artefact which mimics an extended source for ultra-soft photons. Compared with the ROSAT PSPC the spatial resolution of the HRI detector is higher by about a factor of ~ 5. The HRI therefore is more suitable to search for an extended emission component on small angular scales. Inspecting the 1994 HRI data we found a small elongation of the pulsar's X-ray counterpart towards a direction of $105 \pm 5°$ measured anticlockwise from north. Since this orientation is consistent with the satellites wobble direction ($\sim 102°$) we conclude that this elongation is an artefact of uncorrected residual wobble rather than a feature associated with the pulsar's H_α nebula. To prevent such a source extension due to incomplete attitude correction we observed the pulsar in 1997 with the satellite wobble disabled. Figure 3 shows the HRI image of the pulsar field based on the 1997 data. As can be seen from this image there is no indication of an ellipsoidal elongation in the orientation of the optical bow-shock nebula as found in the 1994 HRI data. Figure 4 shows that the source extent of the pulsar's X-ray counterpart is in agreement with the ROSAT HRI point-spread-function (see also Boese 1998).

To search for a possible X-ray emission component from the side wings of the bow-shock nebula we used the merged 1994 and 1997 HRI data. 785 counts were selected from within three quarter of a ring around PSR J0437−4715, having an inner radius of 12" and and outer radius of 60" in the orientation of the optical image of the pulsar bow-shock. Figure 5 shows the selected sky region scaled up by a factor 6 compared with Fig. 3. Its area is approximately 2.6 arcmin^2, implying a surface brightness of $\sim$ 302 cts arcmin^{-2}. Shifting the mask to source free regions in the neighborhood of PSR J0437-4715 we find that on average 642 of the 785 counts in the mask belong to the background. The excess of 143 counts above the background level is about 6% of the $\sim$ 2480 pulsar counts falling within the 12 arcsec inner radius of the mask and thus is well explained by mirror scattering (David et al. 1997). For the 3σ count rate upper limit of a diffuse nebula component we find $3 \times \sqrt{785}/58\,138$ cts/s $= 1.4 \times 10^{-3}$ cts/s (see Becker 1995, p65). Assuming a power-law spectrum with a photon-index $\alpha = -2$ and a column density of $N_H = 0.8 \times 10^{20}$ cm^{-2} (see Sect. 4.3) the count rate upper limit corresponds a 3σ flux upper limit of $< 5 \times 10^{-14}$ erg s^{-1} cm^{-2} and a luminosity of $< 2 \times 10^{29}$ erg s^{-1} $(d/180\mathrm{pc})^2$ in 0.1−2.4 keV. Com-

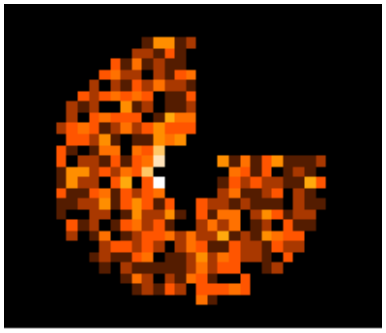

Fig. 5. Sky region around PSR J0437−4715 selected to quantify a possible X-ray emission component from the side wings of the pulsar's bow-shock nebula. The mask has an inner radius of 12" and and outer radius of 60" in the orientation of the optical image of the pulsar bow-shock. The pixel size is 5x5 arcsec. Based on the merged 1994 and 1997 HRI data we find in total 785 counts within the covered area.

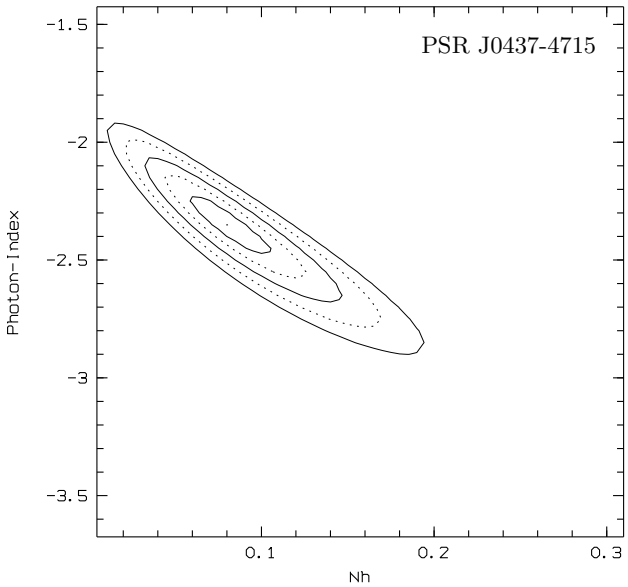

Fig. 6. Contour plot of χ^2 as a function of the Galactic column density $N_H \times 10^{21}\,\mathrm{cm}^{-2}$ and the photon-index α. The confidence levels range from 1σ to $5igma$.

pared with the pulsar's spin-down energy this is less than $0.2 \times 10^{-3}\,\dot{E}$, similar to the 3σ conversion upper limit found for a possible bow-shock contribution to the X-ray emission from 1957+20 (Fruchter et al. 1992).

4.3. Spectral emission properties

Becker & Trümper (1993) have shown that the pulsar's soft X-ray spectrum in 0.1−2.4 keV is best described by a power-law $dN/dE \propto E^{\alpha}$. Figure 6 shows the χ^2 contour plot of this model in the $N_H - \alpha$ plane. The best fitting parameters for this model, deduced from the merged 1992 and 1994 PSPC data, are a column density $N_H = (8 \pm 2.5) \times 10^{19}\,\mathrm{cm}^{-2}$ and a photon-index of $\alpha = -2.35 \pm 0.15$. This is in agreement with the results found by Halpern et al. (1996) based on a combined EUVE/ROSAT spectral analysis using the Sep. 1992 data only. The 1994 PSPC data taken with the Boron filter[2] were used for a cross check of the fitted power-law spectral parameters by computing the count rate ratio for an observation with and without a Boron filter and comparing this with the measured value. The result was found to be in agreement with the filter-off spectral fittings.

The pulsar's energy flux deduced from the best fitting power-law model is $f_x = 1.9 \pm 0.2 \times 10^{-12}\,\mathrm{erg\ s^{-1}cm^{-2}}$ in 0.1−2.4 keV, implying an X-ray luminosity of $L_x = 7.3 \pm 0.8 \times 10^{30}\,\mathrm{erg\ s^{-1}}\,(d/180\mathrm{pc})^2$ and a conversion factor of $L_x/\dot{E} \cong 4 \times 10^{-3}$.

It was already shown by Becker & Trümper (1993) that a single black-body spectrum does not fit the ROSAT data and leaves a residual hard excess above ~ 0.5 keV (see also Becker 1995, p125), whereas a double black-body model yields acceptable spectral fits. Based on ASCA observations, Kawai et al. (1998 – hereafter KTS98) have reported recently that the pulsar spectrum beyond 0.7 keV fits better with a black-body rather than with a composite (power-law plus black-body) or simple power-law spectrum. The authors deduced a temperature of $T \sim (3 \pm 0.5) \times 10^6$ K, a black body radius of $R_{bb} \sim 54\,\mathrm{m}\,(d/180\,\mathrm{pc})$ and a bolometric flux of $f_{bb} \sim 5.1 \times 10^{-13}\,\mathrm{erg\ s^{-1}\,cm^{-2}}$. Figure 7a shows the ROSAT PSPC data fitted with a double black-body spectrum in which the parameters of the second (harder) spectral component have been fixed according to the ASCA results. The parameters of the soft black-body component have been fitted and imply a temperature of 1.2×10^6 K, $R_{bb} \sim 510\,\mathrm{m}\,(d/180\,\mathrm{pc})$ and a bolometric flux of $f_{bb} = 8.6 \times 10^{-13}\,\mathrm{erg\ s^{-1}\,cm^{-2}}$. The column density in this model is fitted to be zero. Due to the small radii both black-body components are attributed to the pulsar's polar cap. The X-ray flux detected with ASCA above 0.7 keV is not pulsed. The authors give a pulsed fraction upper limit of 70%.

An alternative to the double black-body model, also suggested by KTS98, is that the simple power-law component seen by ROSAT and EUVE has a spectral break near the upper boundary of the ROSAT band. In fact, the authors found that both a broken power-law model or a power-law model with exponential cut-off can describe the X-ray data from PSR J0437−4715 very well. The ASCA data imply a spectral break (cut-off) near ~ 1.4 keV with a slope of about -4 for the second power-law component. The broken power-law model fitted to the

[2] The advantage of the Boron filter is to improve the PSPC's spectral resolution in the carbon band ($0.1 - 0.288$ keV) by a further subdivision of this energy range into two bands. See Stephan et al. 1991 for informations on the filter transmission.

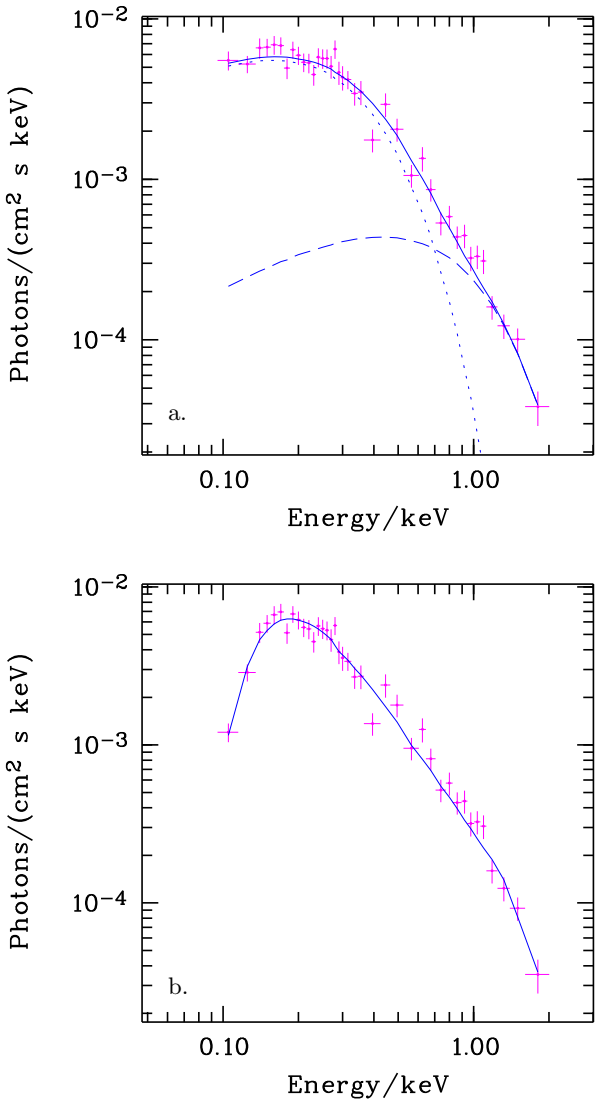

Fig. 7. a. The ROSAT PSPC data of PSR J0437−4715 fitted with a two component black body model. The harder component (dashed line) represents the black-body spectrum as deduced from spectral fits to ASCA data (see text). The dotted line represents the soft component as obtained from a spectral fit to the ROSAT data. **b.** The PSPC data fitted with a broken power-law. The break energy in this model is 1.4 keV. The slopes of the first and second power-law components are −2.35 and −4.5, respectively.

ROSAT data is shown in Fig. 7b. The slopes of the first and second power-law components are -2.35 ± 0.15 and -4.5 ± 1.65, respectively. The column density is found to be $N_H = 0.8 \times 10^{20}\,\mathrm{cm}^{-2}$.

A number of different spectral models which assume thermal emission from polar hot spots taking into account the influence of a possible neutron star H-, He- or Iron-atmospheres have been tested recently for PSR J0437−4715 by several authors (see Rajagopal & Romani 1996; Pavlov et al. 1996; Zavlin & Pavlov 1998). All these models yield spectral fits which are in a somewhat better agreement with the data than a simple black-body spectrum but still leave some unmodeled hard excess above 1 keV. The polar cap model of Zavlin & Pavlov (1998) predicts a pulsed fraction of more than 50% for the emission above 1.1 keV, in contradiction to what is observed with ROSAT (see Sect. 4.4 and Table 1).

Table 1. Temporal emission properties of PSR J0437-4715

Data set	Range [keV]	Source cts	Bg cts	Pulsed cts	PF [%]
PSPC 1992	0.1 − 2.4	1200	24	326 ± 48	28 ± 4
	0.1 − 0.6	896	19	232 ± 38	27 ± 4
	0.6 − 1.1	211	3	67 ± 19	32 ± 9
	1.1 − 2.4	102	2	16 ± 14	18 ± 14
PSPC 1994	0.1 − 2.4	2001	80	588 ± 74	29 ± 4
	0.1 − 0.6	1594	67	410 ± 59	27 ± 4
	0.6 − 1.1	363	10	107 ± 33	30 ± 9
	1.1 − 2.4	158	8	27 ± 20	16 ± 14
Boron	0.1 − 2.4	145	4	37 ± 13	26 ± 9
HRI-94*	0.1 − 2.4	1055	9	300 ± 50	29 ± 5
HRI-97	0.1 − 2.4	985	12	256 ± 40	26 ± 4

Errors represent the 1σ confidence range.
*Based on data taken on 21. and 22. Aug. 1994

4.4. Temporal emission properties

Because of the long time gap between the two PSPC observations and the difference in detector type between the HRI and PSPC we have analyzed the available ROSAT data from PSR J0437−4715 independently of each other. The results can therefore be regarded as independent measurements. In the following we give a detailed description of the data analysis for the different data sets.

Quantities such as the number of counts, the background contribution and the number of pulsed counts as well as the fraction of pulsed photons for different energy ranges are summarized in Table 1.

4.4.1. The 1992 PSPC data

A timing analysis based on this data but using a preliminary pulsar ephemeris led to the discovery of the X-ray pulses from PSR J0437−4715 by Becker & Trümper (1993). The results of a reanalysis were presented recently by Halpern et al. (1996) using an improved ephemeris. However, to perform a timing analysis consistently for all five data sets we have analyzed the PSPC-92 data again using a pulsar ephemeris valid at an epoch close to the ROSAT observational epoch.

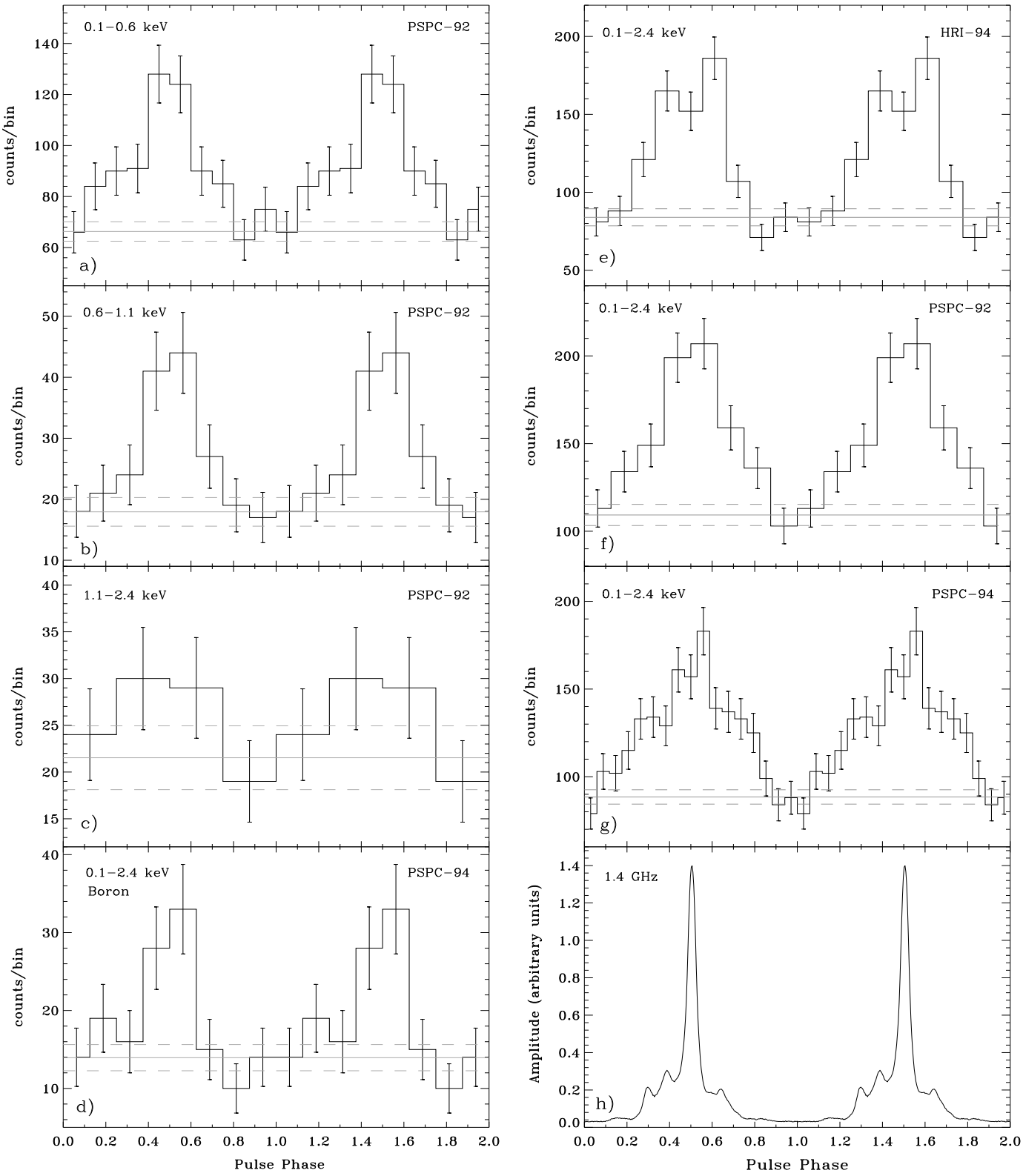

Fig. 8. Integrated pulse profiles of PSR J0437-4715 for different energy ranges. Two phase cycles are shown for clarity and 1σ errors are indicated. Panels **a-c** depict the profiles based on the 1992-PSPC data. Panels **d-g** show the pulse profiles within the full ROSAT energy range taken with the HRI in 1994 (e) and the PSPC in 1992 and 1994 (d,f,g), respectively. The DC-level and its 1σ error is indicated by solid and dashed lines, respectively. No phase shift is observed for the pulses within the ROSAT energy band. The X-ray pulses are found to be consistent with a constant pulsed fraction and a pulse shape which appears similar to the radio one shown in panel **h** (see text and Table 1 for details). The relative phase between the X-ray and radio profiles in this figure has been fixed arbitrarily (see Sect.4.4.4).

For the photon arrival time analysis of the 1992-PSPC data we have selected 1200 photons from an 70 arcsec aperture centered on the pulsar's X-ray position. The cut-radius was chosen according to the PSPC's point-spread function and contains more than 99.9% of the pulsar counts. 70 arcsec is large enough to select most of the ultra-soft photons subject to the electronic ghost-imaging effect (Briel et al. 1996) which is barely present in this data set. An extraction radius of $\sim$ 100 arcsec as used by Halpern et al. (1996) appears too large and selects an unnecessary large fraction of background photons.

The folded pulse profiles for different energy ranges are shown in Fig. 8a−c. The H-Test yields the highest probability for 2 harmonics, indicating a small deviation from a sinusoidal shape. The width of the X-ray pulse is approximately 0.8 rotations ($\approx 290^\circ$), practically the same as observed in the radio domain (see Fig.8h). The fraction of pulsed photons, measured for the different energy ranges by using the bootstrap approach is given in Table 1. There is no significant pulsed X-ray emission above 1.1 keV in the 1992-PSPC data (see Fig.8c). Only 102 photons have been detected in this energy range, for which the bootstrap method indicates a pulsed fraction of $18 \pm 14\%$. In contrast to our earlier findings (Becker & Trümper 1993) the bootstrap method indicates that the pulsed fraction is independent of the photon energy in the ROSAT band.

4.4.2. The 1994 PSPC data

In contrast to the 1992-PSPC data, we find that the spatial extent of the pulsar's X-ray counterpart below ~ 0.25 keV is strongly dominated by the electronic ghost-imaging effect. In order not to exclude these ultra-soft photons from the analysis we have selected the pulsar counts below 0.25 keV from an extended region chosen according to the expected pattern of photon imaging (Briel et al. 1996). The PSPC count rate from this area yields a rate of 0.205 ± 0.005 cts/s, in agreement with the count rate observed in the 1992-PSPC data (Becker & Trümper 1993). In total, we have selected 2101 counts for the timing analysis, more than 99% of the total pulsar contribution. Folding the corrected and barycentered arrival times with the pulsar's rotation frequency resulted in the pulse profile shown in Fig.8g. The pulse profiles obtained for the energy ranges 0.1−0.6 keV, 0.6−1.1 keV and 1.1−2.4 keV are not significantly different from the profiles shown in panel 8a-c. The pulse profile obtained from the observation using the boron filter is shown in Fig. 8d.

4.4.3. The 1994 and 1997 HRI data

As already pointed out in Sect. 4.1, the pulsar's 1994 HRI observation of $\sim$ 35 000 s is distributed over a period of 38 days. Approximately 9800 s of the exposure time was taken between July 18th and August 13th 1994 whereas about 25 300 s of the exposure was taken within only two days on August 21-22. Selecting the photons from an aperture of 10 arcsec radius centered on the pulsar yielded 1484 counts available for the timing analysis. These are approximately 90% of all pulsar counts and a background contribution of only $\approx 1\%$. Folding the arrival times with the pulsar's rotational frequency (using the same ephemeris as already used for the timing analysis of the 1994-PSPC data) we find from the H-Test that the significance for pulsations is maximized for 3 harmonics at $Z_3^2 \approx 91$, indicating a somewhat stronger deviation from a sinusoidal pulse shape than previously found in the PSPC data. However, the fraction of pulsed photons is found to have a rather low value of only $20 \pm 4\%$. For a consistency check we have therefore performed the same analysis again but at this time restricted to the data taken on 1994 August 21. and 22. only. The result is interesting in the sense that we find both the significance of the pulsed signal and the fraction of pulsed photons enhanced to $Z_3^2 \approx 120$ and $29 \pm 5\%$, respectively, although the number of source counts available for the analysis is reduced to 1055. The shape of the pulse profile found in both data sets is not significantly different and shows only a change in the DC level. The profile based on the 21−22 August 94 data is shown in Fig.8e.

The differences in significance and pulsed fraction are probably due to the limited stability of the ROSAT onboard clock having a nominal drift of $\approx 8 \times 10^{-8}$ per day. At the pulsar's observational epoch, clock calibration measurements were only performed once per week. Investigating the residuals of a linear fit from the space craft clock calibration against UTC we find a change in the drift rate approximately in the middle of the first half of the 1994 HRI observation whereas the drift rate stays nearly constant for the remaining time of the observation. From this we conclude that folding all data from the full 38 day observation span results in a smearing of the pulsed emission leading to a reduction of the pulsed fraction. We conclude that the pulsed fraction of $29 \pm 5\%$ for the 1994 HRI data is in agreement with the results of the two PSPC observations.

For the HRI data taken in September 1997 we applied the same analysis as for the 1994 data. The results are in agreement with findings deduced from the 1994 HRI observation (see Table 1).

4.4.4. Relative phase between the X-ray and radio pulse

In view of the short pulse period of millisecond pulsars and the uncertainty in the ROSAT space craft clock calibration against Coordinated Universal Time (UTC), a comparison of the relative phase between the X-ray and radio pulses for PSR J0437−4715 appears difficult. Calibration measurements of the satellite's space craft clock against UTC are available with a frequency of usually once per week for the pulsar observational epochs in 1992 and 1994. A daily clock calibration has been performed only since November 1996.

In order to measure the X-ray pulse arrival relative to the radio pulse we made local fits to the ROSAT clock calibration points against UTC using three and four order polynomial functions. With this approach we find residuals which are in the order of $1-2$ ms. Although this surely represents the limits of the clock accuracy against UTC it still corresponds to a relative error in the X-ray pulse arrival time of approximately $20-30\%(1\sigma)$. In view of these uncertainties the relative phase between the radio and X-ray pulse of PSR J0437-4715 cannot be constrained with the available ROSAT data. More accurate timing will be available on AXAF and XMM, which will provide the desired information.

5. The globular cluster pulsar B1821-24 in M28

PSR B1821−24 is an isolated 3.1 ms pulsar in the globular cluster M28. Among the few tens of known millisecond pulsars it has the highest spin-down energy. X-ray emission from the source was detected with the ROSAT PSPC in March 1991 (Danner et al. 1994) and with the ROSAT HRI and the ASCA GIS & SIS detectors in March 1995 (Danner et al. 1997; Saito et al. 1997). The results of these observations are remarkable in the sense that they detect pulsed X-rays in the wide energy band from 0.1−10 keV.

Figure 9 shows the X-ray and radio pulse profile as observed with the ROSAT HRI (top profile), the ASCA GIS-detector (middle profile) and the National Radio Astronomy Observatory in Green Bank (bottom profile). The X-ray light curves are double peaked with a very narrow profile for the pulse components. The significance of the X-ray pulses is about 4σ in the HRI data.

The high resolution pulse profile observed at 800 MHz was published recently by Backer & Sallmen (1997). At this frequency, the radio profile shows three pulse components, of which peak #2 is found to show intensity variations on time scales of hours to days. Backer & Sallmen (1997) found that the spectral-index of the third and broad radio pulse component is similar to the one observed for the narrow and leading pulse component #1. The spectral-indices measured between 470 - 1700 MHz are -1.4 ± 0.2 and -3.1 ± 0.2 for the first and second pulse component (Foster et al. 1991).

Unfortunately neither the ROSAT nor the ASCA clock calibration is sufficient to phase relate the X-ray pulses of a 3.1 ms pulsar with the radio pulse. However, recent observations of PSR 1821−24 with the Rossi X-ray Timing Explorer (Rots et al. 1997) have shown that the primary X-ray pulse component appears to be nearly phase aligned with the radio pulse component dominating at 800 MHz. Phase alignment between radio and X-ray pulses is only established (with sufficient accuracy) for the Crab pulsar. Unless the phase alignment is chance coincidence it suggests a common emission site for both the main radio and the dominating X-ray pulse.

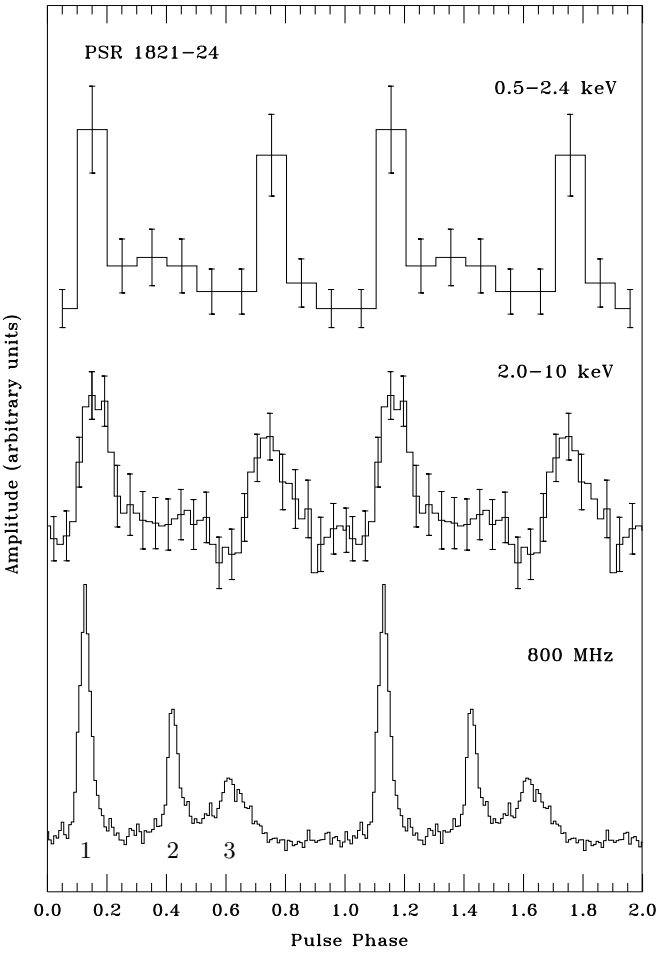

Fig. 9. Integrated pulse profiles of the globular cluster pulsar PSR 1821−24 as observed with the ROSAT HRI (top) by Danner et al. (1997), the ASCA GIS detector by Saito et al. (1997) and with the NRAO at 800 MHz (bottom) by Backer & Sallmen (1997). Two phase cycles are shown for clarity. The X-ray pulse profiles are characterized by a double peak structure with a phase separation of ~ 0.6 between the two peaks. The radio profile at 800 MHz depicts three pulse components. At this frequency the dominating radio pulse is nearly phase aligned with the primary X-ray pulse.

The spectral analysis based on the ASCA data shows that the pulsars' X-ray spectrum between $0.7-10$ keV is well described by a power-law with a phase averaged photon-index of about $\alpha \approx -2$ (Saito et al. 1997). The first and the second pulse show photon-indices of -1.5 ± 0.3 and -2 ± 0.3, respectively. The spectrum of the globular cluster emission, which is assumed to be the interpulse emission, is not well constrained. The interpulse emission appears to be softer than the pulsar emission, but the data do not allow us to discriminate between several possible spectral models: a power-law with a photon-index of -2, an optically thin thermal model with kT=1.4 keV and

a kT=6.2 keV bremsstrahlung model yield all acceptable fits.

Imaging M28 with the ROSAT HRI has shown two separate sources: the point source RX J1824.5-2452P consistent with the millisecond pulsar position and a brighter extended source RX J1824.5-2452E, whose nature is not yet clear (Danner et al. 1997). The presence of the two objects, unresolved by ASCA, further confuses the spectral interpretation. The power-law spectrum of the interpulse data (i.e. the spectrum of the extended source RX J1824.5-2452E) favors the model in which RX J1824.5-2452E is a pulsar powered synchrotron nebula, similar to the Crab. An alternative and may be more likely interpretation, however, is that RX J1824.5-2452E is made of a number of point sources (e.g. accreting binaries containing white dwarfs or neutron stars) which could not been spatially resolved by the HRI. An interpretation in terms of low accretion LMXBs is also supported from a long term X-ray luminosity study of M28. Our reanalysis of the archival PSPC and HRI data, taken in March 1991 and 1995, suggest an X-ray flux variability of M28 on time scales of years. The total ROSAT HRI energy flux taken in March 1995 from M28 is about a factor of 3 higher than the total energy flux deduced from the March 1991 PSPC observation. This behavior is in line with the results recently published by Gotthelfe & Kulkarni (1997) who discovered an X-ray burst from M28 in the 1995 ASCA data.

Estimating the pulsar's energy flux and luminosity from the HRI count rate ($3.7 \pm 0.4 \times 10^{-3}$cts/s) yields for the power-law spectrum $f_x = (5.2 \pm 0.6) \times 10^{-13}$ erg s^{-1}cm^{-2} and $L_x = 1.6 \pm 0.2 \times 10^{33} (d/5.1 \text{ kpc})^2$ erg s^{-1} within 0.1−2.4 keV, respectively. The latter implies an X-ray efficiency of $L_x/\dot{E} \approx 0.8 \times 10^{-3}$. For the interstellar absorption we used $N_H = 2.8 \times 10^{21}$ cm^{-2} which is consistent with the ASCA measurements (Saito et al. 1997) and the column density deduced from the dispersion measure.

6. PSR J0218+4232

The 2.3 ms pulsar PSR J0218+4232 was discovered by Navarro et al. (1995). The pulsar is in a two day binary orbit with a low-mass white dwarf companion and shows significant *unpulsed* radio emission throughout the pulse period. The latter has been taken by Navarro et al. (1995) as an indication that the magnetic dipole is almost aligned with the rotation axis. The Taylor & Cordes model indicates a dispersion measure based distance of 5.7 kpc.

X-rays from the pulsar were detected on the basis of ROSAT HRI observations by Verbunt et al. (1996). Our re-analysis of the archival ROSAT data confirms their findings. Approximately 47 source counts were recorded from PSR J0218+4232 during the 22 035s HRI observation in August 1995, implying a count rate of $(2.1 \pm 0.4) \times 10^{-3}$ cts/s. This HRI observation was performed ~ 12 arcmin off-axis, resulting in a reduced spatial resolution and point source sensitivity. The source is also marginally detected in a serendipitous ≈ 25 ksec PSPC observation near the edge of the detector's field of view.

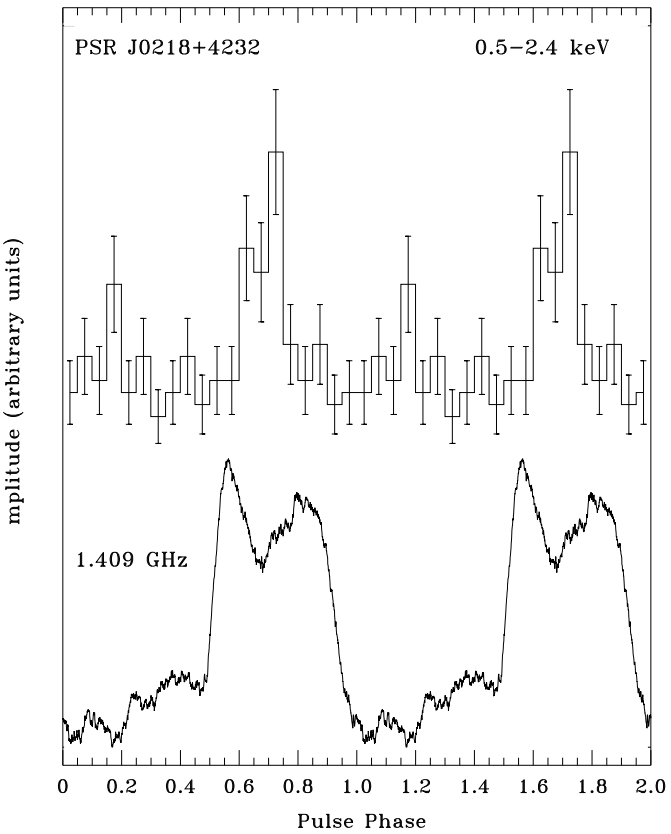

Fig. 10. The X-ray and radio pulse profiles of PSR 0218+4232 as observed with the ROSAT HRI (top) by Kuiper et al. (1998) and with the Effelsberg radio telescope at 1409 MHz (bottom) by Lange et al. (1998, in prep.). Two phase cycles are shown for clarity. The relative phase between the X-ray and the radio pulse is unknown. In this plot it has been arbitrarily fixed.

X-ray pulses from PSR J0218+4232 have been detected only recently using data from a subsequent ROSAT HRI observation which was performed in July 1997 (Kuiper et al. 1998). About 182 source counts were recorded during an exposure time of 98096 s which revealed the existence of a pulsed signal with a statistical significance of $\sim 5\sigma$ and a pulsed fraction of $37 \pm 13\%$. The integrated pulse profiles observed between 0.1-2.4 keV and in the radio channel at 1409 MHz are shown in Fig. 10. As for PSR 2124-3358 (see Sect. 7) there is some indication for the existence of two pulse components in the X-ray lightcurve. Kuiper et al. (1998) mention that the 1998 ROSAT HRI data reveal some marginal evidence for the existence of a compact synchrotron nebula surrounding the pulsar. The authors found in their analysis a source extent of about 14 arcsec. However, the HRI point spread function (PSF) assumed by Kuiper et al. (1998) may have been underestimated by neglecting systematic uncertain-

ties in the HRI-PSF due to incomplete attitude correction (see Boese 1998 and discussion therein).

No information on the pulsars X-ray spectrum is available so far. The HRI provides no spectral information and the number of counts recorded in the serendipitous PSPC observation foes not allow spectral modeling. An estimate of the energy flux and luminosity obtained from the HRI count rate yields $f_x = 1.5 \times 10^{-13}$ erg s^{-1}cm^{-2} and $L_x = 5.7 \times 10^{32}\,(d/5.7\ \mathrm{kpc})^2$ erg s^{-1} in 0.1−2.4 keV, implying an X-ray efficiency of $L_x/\dot{E} \approx 2.3 \times 10^{-3}$. The pulsed energy flux is found to be $f_{xp}^{puls} = (3.9 \pm 1.4) \times 10^{-14}$ erg s^{-1}cm^{-2} (Kuiper et al. 1998). The interstellar absorption was adopted from Verbunt et al. (1996) who used the maximum color excess $E(B-V) = 0.09$ (Burstein & Heiles 1982) in the direction of PSR J0218+4232; $A_V = 3.1E(B-V)$ and $N_H = 1.79\times10^{21}\ A_V$ (Predehl & Schmitt 1995) which results in $N_H \approx 0.5 \times 10^{21}$ cm^{-2}.

Although the second EGRET catalog lists a source whose 80% confidence contour contains the millisecond pulsar (Thompson et al. 1995; Verbunt et al. 1996), the third EGRET catalog (Hartman et al. 1998) which is based on more viewing periods and better data statistics than the 2EG catalog invalidates this putative identification. Figure 11 depicts the likelihood map of the sky region around PSR J0218+4232 based on the third EGRET catalog (Hartman et al. 1998). The position of the millisecond pulsar and the gamma-ray source appear well separated from each other. Therefore, the millisecond pulsar PSR J0218+4232 is very unlikely the counter part of the neighboring gamma-ray source 3EG J022+4253 which is identified now with the AGN 3C66A (Hartman et al. 1998).

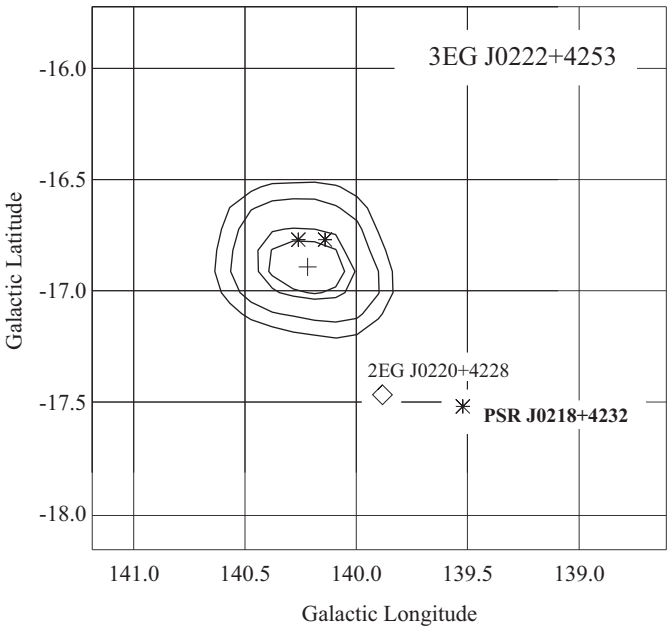

Fig. 11. Confidence regions (50%, 68%, 95%, 99%) of the likelihood test statistics for the position of the EGRET source neighboring the millisecond pulsar PSR J0218+4232. Also shown is the position of the gamma-ray source as listed in the second EGRET catalog (2EG J0220+4228) and the position of the millisecond pulsar. The location of the gamma-ray source is now in agreement with the position of two AGNs, of which 3C66A is found to be the likely counterpart of 3EG J0222+4253 (see Hartman et al. 1998 for further details).

7. The isolated millisecond pulsar J2124−3358

PSR J2124−3358 belongs to the small group of isolated millisecond pulsars. Like PSR J1024−0719 and J1744−1134, it was discovered by Bailes et al. (1997) during the Parkes 436 MHz survey of the southern sky. The pulsar has a rotation period of 4.93 ms and a proper motion corrected period derivative of $\dot{P} = 1.077 \times 10^{-20}$ s s^{-1}, implying an upper limit to the pulsar age of $P/2\dot{P} = 7.3 \times 10^9$ years and a rotational energy loss of $\dot{E} = 3.545 \times 10^{33}$ erg s^{-1}. Its close distance of about 250 pc in combination with spin-parameters similar to that of PSR J0437-4715 made the pulsar a promising candidate for X-ray observations.

ROSAT HRI observations of PSR J2124−3358 were therefore performed on November 3-7, 1995 with an effective exposure time of 88 488s. Figure 12 depicts a 16×16 arcmin^2 sub-image of the pulsar field. The pulsar is visible as the X-ray point source RX J212443.5-335841 at the center of the field. A spatial analysis reveals a positional offset between the pulsar's timing position and its X-ray counterpart of 4.8″, well within the uncertainty of the satellites pointing accuracy. The HRI count rate of PSR J2124−3358 is $(2.6 \pm 0.2) \times 10^{-3}$ cts/s.

We applied a timing analysis to 243 photons selected from an 8″ aperture centered on the pulsar's X-ray position. This *cut* radius includes approximately 97% of the source photons (David et al. 1997). About 10% of the selected photons are background photons. After correcting the data for the satellite's motion and applying a barycenter correction, a folding of the photon arrival times implies strong evidence for the existence of a pulsed signal. The resulting light curve is shown in Fig. 13. According to the H-Test the pulsations are significant at the $\sim 4\sigma$ level (for two harmonics). This establishes RX J212443.5-335841 as the pulsar's X-ray counterpart and shows the source to be the first galactic solitary millisecond X-ray pulsar.

The pulsar's X-ray light curve shows some indication for a double peak as observed in the radio profile at 436 MHz. Both in the radio and the X-ray profile the phase separation between the two peaks appears to be the same. Using the bootstrap method the fraction of pulsed X-ray photons is estimated to be 33 ± 8%.

For a comparison between the relative phases of the X-ray and radio pulses we have fitted the ROSAT clock against UTC for the days $261 - 324$ of the year 1995, i.e.

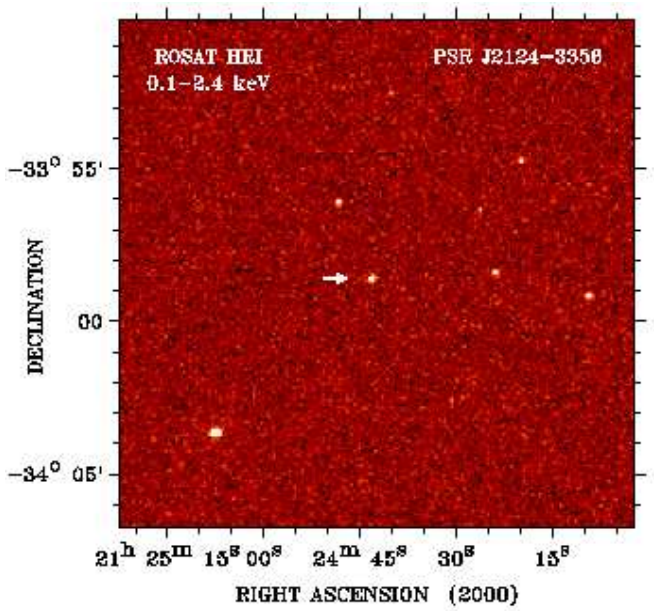

Fig. 12. Sub-image of the HRI's field of view based on the November 1995 ROSAT observation of PSR J2124−3358. The pulsar's X-ray counterpart RX J212443.5-335841 is indicated by an arrow. Several neighboring X-ray sources are detected only few arcmin from the pulsar position.

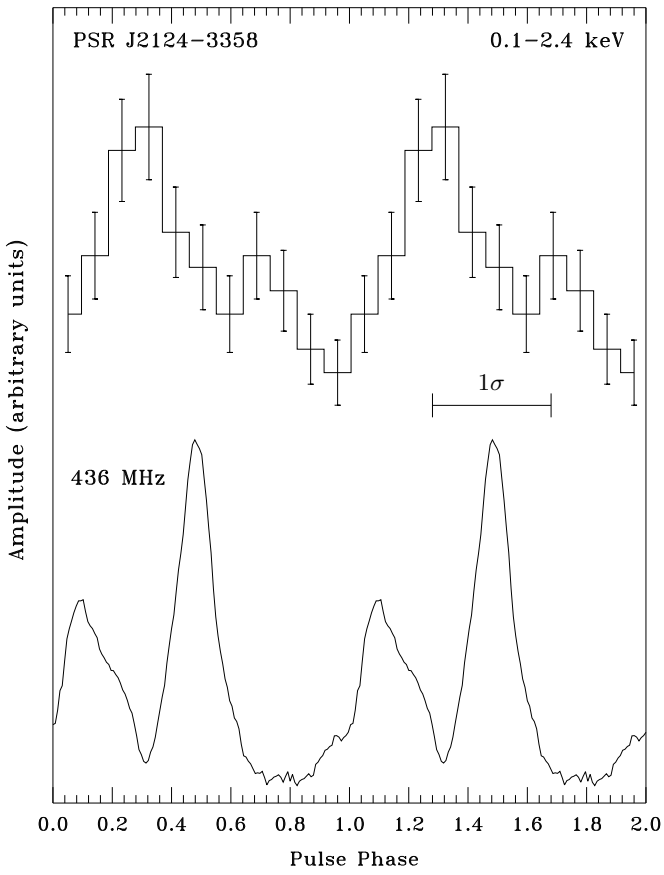

Fig. 13. Light curves of PSR J2124-3358 as observed with the ROSAT HRI in 0.1−2.4 keV (top) and the Parkes radio telescope at 436 MHz (bottom). Two phase cycles are shown for clarity. Both light curves are characterized by two peaks which are separated by ~ 0.4 rotations.

for a period of 9 weeks. This is long enough to model the long term clock drift and to cover the observation which was performed during days $307 - 311$ of 1995. On the other hand we are not limited by clock uncertainties which might have happened long before or after the pulsar observation. Calibration measurements are available close to the pulsar observation on days 303 and 310 of 1995. The residuals of our SCC−UTC fit were found to be of the order of ± 1 ms, corresponding to a 1σ error in the relative phase of 20%. In view of this error it is not possible to draw a quantitative conclusion concerning the phase relation between the X-ray and radio pulse of PSR J2124−3358. However, one may speculate that the similarity of both profiles with respect to the phase separation of 0.4 between the pulse components may suggest a phase alignment of the dominant radio pulse with the weak X-ray pulse.

Assuming a power-law spectrum with a photon-index of $\alpha = -2$ the detected HRI rate corresponds to an energy flux of $f_x \approx 2 - 3 \times 10^{-13}$ erg s^{-1}cm^{-2} and an X-ray luminosity of $L_x \approx 1.5 - 2.2 \times 10^{30} (d/0.25 \text{ kpc})^2$ erg s^{-1} in 0.1−2.4 keV. The latter implies an X-ray efficiency of $L_x/\dot{E} \approx 0.4 - 0.6 \times 10^{-3}$. The pulsed luminosity is estimated to be $L_{xp}^{puls} = 6.2 \times 10^{29}$ erg s^{-1}. Based on the radio dispersion measure of 4.6 pc cm^{-3} (Bailes et al. 1997) and the HI in the Galaxy (Dickey & Lockman 1990) the interstellar absorption is estimated to be in the range $N_H \approx 2 - 5 \times 10^{20}$ cm^{-2}.

8. Conclusions

Nine millisecond pulsars are currently detected in the soft X-ray domain. Five of them have been identified only by their positional coincidence with the radio pulsar and in view of their low number of detected counts do not provide much more than a rough flux estimate. These objects are so faint that the high collecting power of AXAF and XMM will be needed to detect enough photons required for a detailed spectral and temporal study in the soft and the hard band beyond 2 keV. More detailed results are found for the other four millisecond pulsars, all of which provide interesting empirical information on the pulsar's X-ray emission mechanisms.

PSR 1821−24 in the globular cluster M28 shows X-ray pulses up to 10 keV. The sharp peaks in the pulse profile and the power-law nature of the spectrum doubtlessly argue for a non-thermal origin of the detected emission. The alignment between the radio and X-ray pulse component adds further support to this interpretation and implies a common emission site for the main X-ray and radio pulse

components observed at 800 MHz. For PSR J0218+3242 the sharp peaks found in the X-ray pulse profile also argue for a non-thermal origin of the emission.

The situation for PSR J2124−3358 and J0437-4715 is not that clear. For PSR J2124−3358 there is some indication of a double peak structure in the X-ray pulse profile, which in terms of pulsed components and pulse phase separation implies a similarity between the X-ray and radio profile observed at 436 MHz. However, the significance of the second peak is not very strong so that further observations are required to establish this similarity. Furthermore, for broad pulse profiles the shape of a profile itself is not a strong indicator for the origin of the detected emission: a radiation cone which yields sharp peaks at one aspect angle may well be seen as hardly modulated away from this angle. While sharp peaks indicate non-thermal emission processes the reversal – soft modulated emission originates from thermal processes – need not be true. The case of PSR J0437-4715 is uncertain as well. Here the bandwidth limitation of ROSAT and the statistical limitations of the ASCA and SAX observations prevent us from conclusively discriminating between multi-component thermal spectra (thermal polar-cap emission) and a non-thermal origin of the radiation.

Putting the observed emission properties of the detected millisecond pulsars in a somewhat wider frame Becker & Trümper (1997) found recently that the X-ray luminosity of the detected millisecond pulsars show the same linear relationship with the same X-ray efficiency as the Crab-like pulsars, indicating that the bulk of their emission is mainly due to non-thermal processes. The occurrence of power-law spectra in PSR B1821−24 and PSR J0437-4715 and the similarity between the radio/X-ray pulse profiles seen also for PSR J0218+4232 and J2124−3358 may be considered as providing additional evidence for a non-thermal origin of the millisecond pulsars' X-ray emission.

In order to better constrain the origin of the X-radiation of the millisecond pulsars reported in this paper, additional observations with better photon statistics are needed. AXAF and XMM, which are designed to have higher sensitivity and better spectral, timing and spatial performance than ROSAT and ASCA are well suited to study millisecond pulsars and to enhance our understanding of these objects in many aspects.

Acknowledgements. The first author wants to thank Okkie de Jager for useful discussions on pulse fraction estimates. We also thank Olaf Reimer for the help with the EGRET data and Bob Hartman for providing the position of 3EG J0222+4253 prior publication. Thanks to Jon Bell, Dick Manchester and Matthew Bailes for the radio ephemeris and pulse profiles of PSR J0437−4715 and PSR J2124−3358, to Don Backer and Yoshitaka Saito for the radio and ASCA light curves of PSR 1821−24 and to Lucien Kuiper for the lightcurve od PSR J0218+4232. Thanks to the Bonner Pulsar Group at MPIfR for supporting us with the 1.4 GHz pulse profile of PSR J0218+4232 prior publication. The ROSAT project is supported by the Bundesministerium für Bildung, Wissenschaft, Forschung und Technologie (BMBW) and the Max-Planck-Society (MPG). We thank our colleagues from the MPE ROSAT group for their support.

References

Alpar M.A., Cheng A.F., Ruderman M.A., Shaham J., 1982, Nat, 300, 728
Arons J., 1981, ApJ, 248, 1099
Arons J., Tavani M., 1993, ApJ, 403, 249
Backer D.C., Sallmen S., 1997, ApJ, 114, 1539
Bailes M., Johnston S., Bell J.F., et al., 1997, ApJ, 481, 386
Bailyn C. D., 1993, ApJ, 411, L83
Becker W., 1995, PHD-thesis, LMU-München, MPE-Preprint 260, p.124ff
Becker W., Trümper J., 1993, Nat, 365, 528
Becker W., Trümper J., 1997, A & A, 326, 682
Becker W., Trümper J., 1998, IAU Circular 6829
Becker W., Trümper J., Brazier K.T.S., Belloni T., 1993a, IAU Circular No. 5701
Becker W., Brazier K.T.S., Trümper J., 1993b, A&A, 273, 421
Becker W., Trümper J., Lundgren S.C., Cordes J.M., Zepka A.F., 1996,MNRAS, 282, L33
Becker W., Trümper J., Hasinger G., 1998, IAU Circular 6845
Bell J.F., Bailes M., Bessel M.S., 1993, Nat, 364, 603
Bell J.F., Bailes M., Manchester R.N., Weisberg J.M., Lyne A.G., 1995, ApJ, 440, L81
Bell J.F., Bailes M., Manchester R.N., et al., 1997, MNRAS, 286, 463
Blandford R., Teukolsky S.A., 1976, ApJ, 205, 580
Bhattacharya D., Van den Heuvel E.P.J., 1991, Phys. Rep., 203, 1
Bisnovatyi-Kogan G.S., Komberg B.V., 1974, SvA, 18, 217
Boese G., 1998, *The ROSAT Point Spread Function and Associates*, available online via `http://wave.xray.mpe.mpg.de/exsas/documentation/tech_reports`
Briel U.G., Aschenbach B., Hasinger G. et al. 1996, ROSAT Users Handbook, available online via `http://ftp.rosat.mpe-garching.mpg.de:80/rosat_svc/doc/handbook/html`
Buccheri R., De Jager O.C., in Timing Neutron Stars, eds H.Ögelman, E.P.J. van den Heuvel, p95, Kluwer Academic Publishers, 1989
Burstein D., Heiles C., 1982, AJ, 87, 1165
Camilo F., 1996, in High Sensitivity Radio Astronomy, ed N. Jackson, Cambridge University Press, in Press
Camilo F., Thorsett S.E., Kulkarni S.R., 1994, ApJ, 421, L15
Cordes J., Romani R.W., Lundgren S.C., 1993, Nat, 362, 133
Danner R., Kulkarni S.R., Thorsett S.E., 1994, ApJ436, L153
Danner R., Kulkarni S.R., Saito Y., Kawai N., 1997, Nat388, 751
Danziger I. J., Baade D., Della Valle M., 1993, ApJ, 408, 179
David L.P., Harnden F.R., Kearns K.E., Zombeck M.V., 1997, The ROSAT HRI Calibration Report, SAO, available online via `http://hea-www.harvard.edu/rosat/rsdc_www/HRI_CAL_REPORT/hri.html`
De Jager O.C., 1987, thesis, Potchefstromm University for Christian Higher Education, South Africa
Dickey J. M., Lockman F. J., 1990, ARA & A., 28,215
Djorgovski S.G., Evans C.R., 1988, ApJ, 335, L61

Fichtel C.E., Bertsch D.L., Hartman R.C., et al., 1993, A & AS, 94, 13
Foster R.S., Fairhead L., Backer D.C., 1991, ApJ, 378, 687
Fruchter A.S., Stinebring D.R., Taylor J.H., 1988, Nat, 333, 237
Fruchter A.S., Bookbinder J., Garcia M.R., Bailyn C.D., 1992, Nat, 359, 303
Gil J.A., Krawczyk A., 1996, MNRAS, 280, 143
Gotthelfe E.V., Kulkarni S.R., 1997, ApJ, 490, L161
Grupe D., thesis, 1996, University of Göttingen
Halpern J.P., 1996, ApJ, 459, L9
Halpern J.P., Martin C., Marshall H.L., 1996, ApJ, 462, 908
Hartman R.C., Bertsch D.L., Fichtel C.E., et al., 1992, BAAS, 24, 1155
Hartman R.C., Bertsch D.L., Bloom C.E., et al., 1998, to appear in ApJS
Johnston S., Lorimer D.R., Harrison P.A., et al. 1993, Nat, 361, 613
Kawai N., Tamura K., Saito Y., 1998, Adv. Space Res. , Vol 21, No 1/2, pp. 213
Kuiper L., Hermsen W., Verbunt F., Belloni T., 1998, to appear in A & A,
Kulkarni S.R., Hester J.J., 1989, Nat, 335, 801
Kulkarni S.R., Phinney E.S., Evans C.R., Hasinger G., 1992, Nat, 359, 300
Kundt W., Schaaf R., 1993, Ap & SpSc, 200, 251
Lundgren S.C., Zepka A.F., Cordes J.M., 1995, ApJ, 453, 419
Navarro J., de Bruyn A.G., Frail D.A., Kulkarni S.R., Lyne A.G., 1995, ApJ, 455, L55
Nicastro L., Lyne A.G., Lorimer D.R., et al., 1995, MNRAS., 273, L68
Pavlov G.G., Zavlin V.E., Becker W., Trümper J., et al.,1996, proceedings of AAS meeting
Predehl P., Schmitt J., 1995, A&A, 293, 889
Rajagopal M., Romani R., 1996, ApJ, 461, 327
Romani R.W., Cordes J.M., Yadigaroglu I.A., 1997, ApJ, 484, L137
Rots A.H., Jahoda K., Macomb et al., 1997, to appear in ApJ(astro-ph/9801251)
Saito Y., Kawai N., Kamae T., et al., 1997, ApJ, 477, L37
Sandhu J.S., Bailes M., Manchester R.N., et al., 1997, ApJ, 478, L95
Snowden S.L., Hasinger G., Jahoda K., et al., 1994, ApJ, 411, 674
Stark A.A., Gammie C.F., Wilson R.W., et al., 1992, ApJS, 79, 77
Stephan K.H., Schmitt J.H.M.M., Snowden S.L., Maier H.J., Frischke D., 1991, Nucl. Instr. and Meth., A303, 196
Swanepoel J.W.H., de Beer C.F., Loots H., 1996, ApJ, 467, 261
Taylor J.H., Cordes J.M., 1993, ApJ, 411, 674
Taylor J.H., Manchester R.N., Lyne A.G., Camilo F., 1995, unpublished work, available by anonymous ftp at [128.112.94.73]:/pub/catalog
Thompson D.J., Bertsch D.L., Dingus B.L., et al., 1995, ApJS, 101, 259
Tsuruta S., 1998, Physics Reports, 292, 1
Urpin V., Geppert U., Konenkov D., 1998, A & A, 331, 244
Verbunt F., Kuiper L., Belloni T., et al, 1996, A & A, 311, L9
Wijnands R., Van der Klis M, Nat, submitted
Zavlin V.E., Pavlov G.G., 1998, A & A, 329, 583
Zimmermann H.U., Becker W., Belloni T., et al., 1994, MPE-Report 244